

Research Article

Log-Aesthetic Curves for Shape Completion Problem

R. U. Gobithaasan,¹ Yip Siew Wei,¹ and Kenjiro T. Miura²

¹ School of Informatics & Applied Mathematics, Universiti Malaysia Terengganu, 21030 Kuala Terengganu, Terengganu, Malaysia

² Graduate School of Engineering, Shizuoka University, Shizuoka 432-8561, Japan

Correspondence should be addressed to R. U. Gobithaasan; gr@umt.edu.my

Received 20 April 2014; Revised 8 July 2014; Accepted 11 July 2014; Published 11 August 2014

Academic Editor: Juan Manuel Peña

Copyright © 2014 R. U. Gobithaasan et al. This is an open access article distributed under the Creative Commons Attribution License, which permits unrestricted use, distribution, and reproduction in any medium, provided the original work is properly cited.

An object with complete boundary or silhouette is essential in various design and computer graphics feats. Due to various reasons, some parts of the object can be missing hence increasing the complexity in designing process. It is therefore important to reconstruct the missing parts of an object while retaining its aesthetic appearance. In this paper, we propose Log-Aesthetic Curves (LAC) for shape completion problem. We propose an algorithm to construct LAC segment and subsequently fit into the gap of the missing parts with C-shape or S-shape. For C-shape completion, we define LAC segment by specifying two endpoints and their respective tangent directions between the gaps while, for S-shape, the user defines an inflection point in between the endpoints. The final section illustrates three examples to showcase the efficiency of the proposed algorithm. The results are further compared with Kimia's method to prove that the algorithm produces equally good result. Additionally, the proposed algorithm provides an extra degree of freedom in which the user would be able to choose the type of spiral that they desire to solve the shape completion problem.

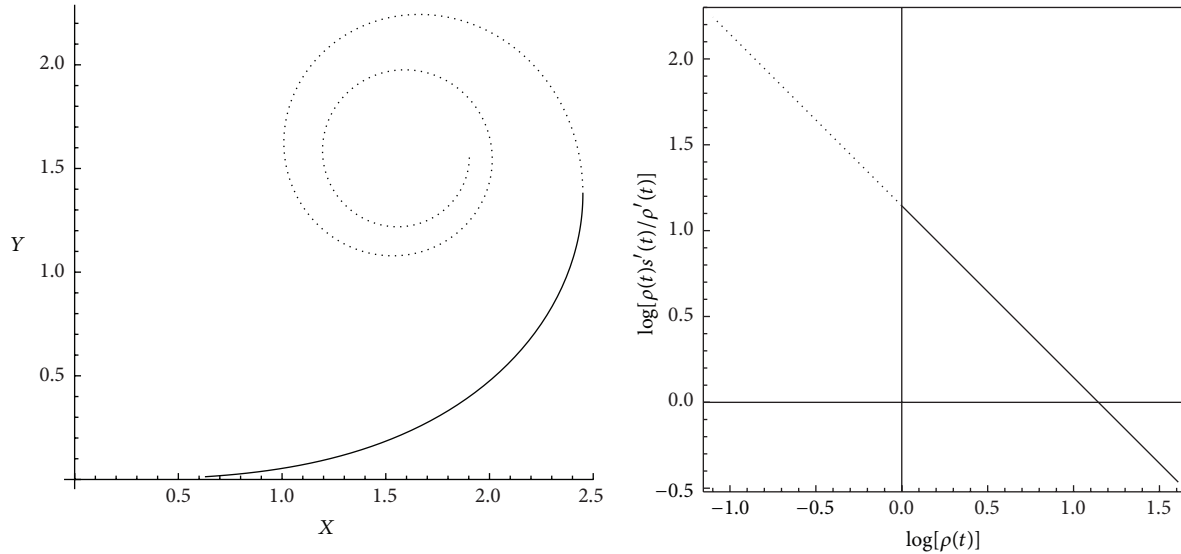
1. Introduction

In a design environment, there are situations in which the outlines of an object are missing or occluded. These scenarios are commonly known as shape completion, gap completion, or curve completion problem. It is important to recomplete the shape of the missing object while retaining its aesthetic appearance since a complete object can be used further for applications in modeling, mesh analysis, and computer-aided design as well as manufacturing purposes. The complete boundary or silhouette provides geometrical information of a model which is significant in engineering analysis and manufacturing process. In order to reconstruct the missing boundaries of an object, the associated curve segment must satisfy the boundary conditions so that the curve passes through the endpoints with specified tangent direction. To date, there are numbers of algorithms available for shape completion problem (see the works of [1–6]).

A notable work which received much attention is by Kimia et al. [3], where they proposed an algorithm which utilizes Euler spiral to solve shape completion problem.

Euler spiral is also known as Cornu's spiral or clothoid. The Euler spiral is widely applied in highway/railway or robotic trajectories design due to its linear curvature property (curvature varies linearly with respect to arc length). The algorithm proposed by Kimia et al. [3] is the implementation of Euler spiral to solve the shape completion problem. In their proposed algorithm, two endpoints (P_0, P_2) and their tangential angles (θ_0, θ_2) are the inputs. In order to construct Euler spiral for the given problem, curvature and arc length of the curve are required to be identified. Since the proposed Euler spiral algorithm is an iterative process, initial guess for these two parameters (curvature and arc length) is needed. Kimia et al. [3] recommended the use of biarc to obtain the initial curve with its corresponding curvature and arc length for the proposed algorithm. Note that the goal of their proposed algorithm is to minimize the distance between last point and resulting curve in order for the gap to be filled using gradient descent method.

Log-Aesthetic Curves (LAC) are curves where the logarithmic curvature graph (LCG) can be represented by a straight line. The idea of LCG was formulated by



(a) Two segments of Euler spiral

(b) Its corresponding logarithmic curvature graph

FIGURE 1: Euler spiral defined $s \in [0.2, 1]$ (solid line) and $s \in [1, 3]$ (dotted) and its corresponding LCG.

Harada et al. (1999) when they attempted to classify all the curves used in automobile design. It was first known as logarithmic distribution diagram of curvature (LDDC). It is a graph to measure the relationship between curvature radius (denoted by ρ) and arc length of the curve segment (denoted by s). They found that all the curves employed in automobile design depict linear gradient of LDDC. Kanaya et al. [7] refined the formulation of LDDC which is now known as LCG. The horizontal axis of LCG represents $\log \rho$ and the vertical axis represents $\log \rho(ds'/d\rho')$ [8]. Figure 1 illustrates the two segments of Euler spiral.

In 2005, Miura et al. [9] derived a fundamental formula of LAC based on a linear representation of LCG. A year later, Yoshida and Saito [10] investigated the characteristics and overall shape of LAC. They also proposed a method to construct LAC segment interactively by specifying endpoints and their tangent vectors. In 2009, they further extended LAC into space curve and proposed a method to interactively control the curves, which is similar to quadratic Bezier curves.

LAC has become a promising curve in graphic and industrial design due to its monotonic curvature property. There are two shape parameters of LAC denoted by α and Λ . The shape parameter α is used to determine the type of spiral within the family of LAC, and Λ is used to satisfy the G^1 constraint during the design process. LAC comprises Euler spiral ($\alpha = -1$), Nielsen spiral ($\alpha = 0$), logarithmic or equiangular spiral ($\alpha = 1$), circle involute ($\alpha = 2$), and others.

In 2011, Gobithaasan and Miura [11] expanded the family of LAC into Generalized Log-Aesthetic Curve (GLAC) by adding generalized Cornu spiral (GCS) to the family of LAC. This includes Euler spiral, logarithmic spiral, circle involute, Nielsen spiral, LAC, and GCS as the members of GLAC.

To note, GCS is proposed by Ali et al. [12] where it becomes Euler spiral when the shape parameter of GCS is zero. GLAC has an extra shape parameter compared to LAC in which it can be used to satisfy additional constraints that occur during design process [13]. The curvature function of GLAC is also monotonic similar to LAC. In 2012, they further extended GLAC into space curve.

In 2012, Ziatdinov et al. [14] defined LAC in the form of incomplete gamma functions. They claimed that this new expression of LAC is capable of reducing the computation time up to 13 times faster. In 2013, the problem of G^2 Hermite interpolation was dealt with by Miura and Gobithaasan [15] by introducing log-aesthetic splines which consists of triple LAC segments. Readers are referred to [16] for a detailed review on aesthetic curves.

In this paper, we introduce the implementation of G^1 LAC algorithm to fit the gap in between the outlines of missing/occlusion objects. We compare the performance of this algorithm with the results obtained by Kimia et al.'s [3] method on the same examples in order to show the effectiveness of LAC to solve shape completion problem.

The rest of this paper is organized as follows. First, the formulation of LAC is reviewed followed by a detailed explanation on the LAC algorithm for solving the shape completion problem. In Section 3, we demonstrate the implementation of the proposed algorithm with various α values with three examples to show the implementation of this method. The data and calculation used in the examples are also depicted in this section. The output of shape completion using Kimia's method is also depicted for comparison purposes. We also make comparison of the results obtained using Kimia et al.'s [3] method and our algorithm. We further show some shape variations which can be obtained by using S-shape LAC in

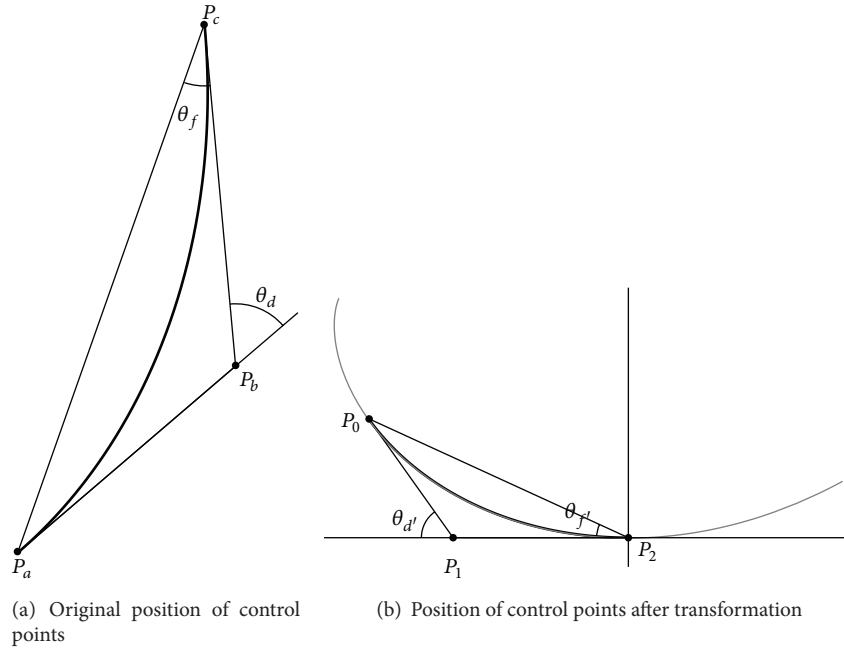


FIGURE 2: The configuration of triangle consists of three control points for case $\alpha > 1$. The curve inside the triangle represents the generated LAC segment.

which the designer tweaks the segment in order to obtain the desired shape.

2. Log-Aesthetic Curves in Shape Completion

In this section, we show the parametric expression of LAC and the algorithm used to obtain the solution for shape completion problem with various α values.

2.1. The Analytical Formulas and Parameters. There are two shape parameters used to define LAC segment: α and Λ . The shape parameter α determines the type of spiral and Λ is used to control the curve so that the constraints are satisfied. Let ρ and θ represent radius of curvature and tangent angle of the curve, respectively.

Equation (1) shows the radius of curvature function in terms of its turning angle. To note, (1) is used to define the parametric expression of LAC in terms of its turning angle as shown in (2) as follows:

$$\rho(\theta) = \begin{cases} e^{\Lambda\theta}, & \text{if } \alpha = 1 \\ ((\alpha - 1)\Lambda\theta + 1)^{1/(\alpha-1)}, & \text{otherwise} \end{cases} \quad (1)$$

$$\text{LAC}(\theta) = P_a + \int_0^\theta e^{iu} \rho(u) du, \quad (2)$$

where P_a represents starting point and i and e represent the imaginary unit and exponent, respectively. LAC can also be represented in the arc length parameter, s , as follows:

$$\text{LAC}(s) = \begin{cases} P_a + \int_0^s e^{i((1/\Lambda)(1-e^{-\Lambda u}))} du, & \text{if } \alpha = 0 \\ P_a + \int_0^s e^{i(\log[\Lambda u + 1]/\Lambda)} du, & \text{if } \alpha = 1 \\ P_a + \int_0^s e^{i(((\Lambda\alpha u + 1)^{(\alpha-1)/\alpha} - 1)/\Lambda(\alpha-1))} du, & \text{otherwise.} \end{cases} \quad (3)$$

Both (2) and (3) generate the same LAC. The curve can be drawn in complex plane by the x -axis representing real numbers and the y -axis representing imaginary numbers. Readers are referred to [10] for a detailed derivation of the parametric expression of LAC.

2.2. The LAC Algorithm

C-Shape. We customize the algorithm of constructing LAC segment to fill the gap by specifying two endpoints, its tangent vector, and α value. The C-shape LAC curve is a direct process in which the user may interactively input the endpoints and the tangent direction of those points. We can further automate the identification of tangents at the endpoints by using three-point circular arc approximation around the endpoints as explained in Steps 1 and 2 in the algorithm below. Using these tangents, we may calculate the midpoint. These three points are then used to fit LAC segment in the gap for shape completion problem. The idea of this method is to find a LAC segment defined in a triangle composed of

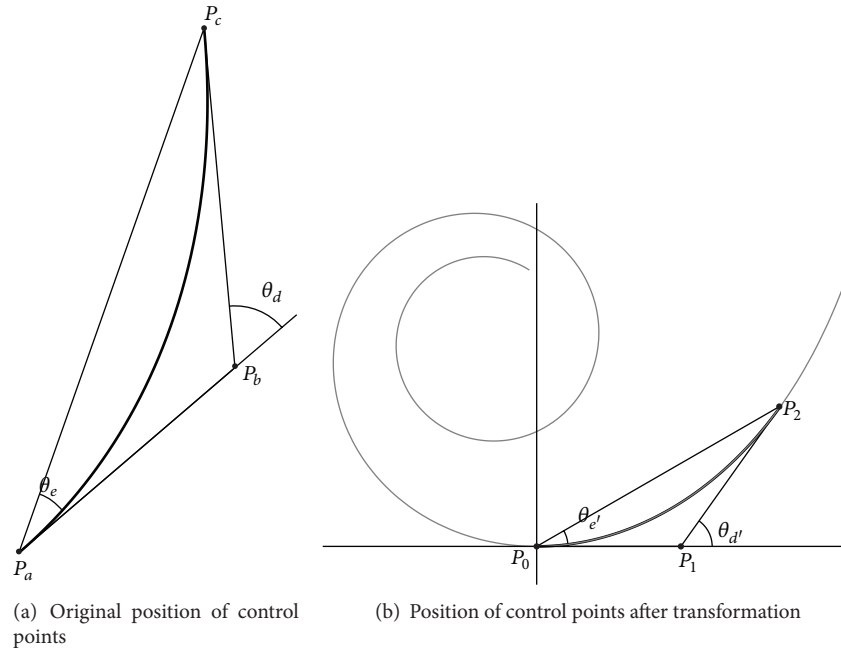


FIGURE 3: The configuration of triangle consists of three control points for case $\alpha \leq 1$. The curve inside the triangle represents the generated LAC segment.

three control points as proposed by Yoshida and Saito [10]. Therefore, by using this method, it is only possible to generate a C-curve. Figures 2 and 3 show the configuration of the triangle formed by three control points for cases $\alpha > 1$ and $\alpha \leq 1$, respectively. Step 5 in the algorithm below elaborates these configurations.

S-Shape. Basically, a S-shape LAC segment consists of two C-shape curves joined with G^1 continuity. In order to construct the S-curve for a given gap, the inflection point is essential. A simple approach used is that users are given the freedom to define the inflection point so that the algorithm is carried out twice consisting of two C-shape segments of LAC. Thus, this approach needs two endpoints, its tangent vectors, α value, and an inflection point.

The process involves breaking the S-curve into two C-curves so the first piece of curve is constructed between starting point (black) and inflection point (gray), while the second piece is between inflection point (gray) and endpoint (black). Figure 4 illustrates the inflection point that we define for one of the numerical examples in this paper.

Algorithm 1 demonstrates the LAC algorithm.

2.2.1. Computation of Tangent Angles (Step 1–Step 3). To automate the process of defining the tangents at the endpoints, we may use circular arc approximation (osculating circle) that best fits the endpoints and points surrounding them in order to determine the tangent angle at both endpoints. Since it is an osculating circle, we substitute the points into the equation of circle. Then, we identify the center (h, k) , radius r , and turning angle t of circle from three points which include



FIGURE 4: The input for S-shape completion problem.

the endpoint. Next, we determine the unit tangent vector at the endpoints and subsequently calculate the corresponding tangent angle by using specified formula as indicated in the algorithm. Alternately, we may also allow the user to directly define tangent vectors at those points.

2.2.2. Identification of Second Control Point (Step 4). Once the unit tangent vector at endpoints is identified, we determine the coordinate of the second control point P_b which is

REMARK: Endpoints $\{P_a, P_c\}$, inflection point P_{infect} and α are user defined. The tangent angle at both endpoints $\{\theta_0, \theta_2\}$ can be obtained either from three point circular arc approximation around the endpoints or the user defines it. Let (X, Y) represent the coordinate of a point.

INPUT: $P_a, P_c, P_{\text{infect}}, \alpha$.

OUTPUT: $\theta_d, \Lambda, r_{\text{scale}}$, LAC segment.

Begin

Step 1. Set $f(t) \leftarrow \{h + r \cos(t), k + r \sin(t)\}$, where (h, k) is the center of circle, r is radius and t represents angle.

Step 2. Identify unit tangent vector, $\text{UTV}(t) \leftarrow f'(t) / \|f'(t)\|$ and set $(X_{\text{new}}, Y_{\text{new}}) \leftarrow (X, Y) + \text{UTV}(t)$.

Step 3. Calculate directional angle, $\theta \leftarrow \tan^{-1}((Y_{\text{new}} - Y) / (X_{\text{new}} - X))$.

Step 4. Solve simultaneous equations $Y = mX + c$, where $m \leftarrow (Y_{\text{new}} - Y) / (X_{\text{new}} - X)$ to get position of second control point P_b .

Step 5. If $\|P_a P_b\| \leq \|P_b P_c\|$, then $P_a \leftarrow P_a; P_c \leftarrow P_c$,

else $P_a \leftarrow P_c; P_c \leftarrow P_a$.

If $\alpha > 1$, then $P_{\text{start}} \leftarrow P_c; P_{\text{end}} \leftarrow P_a$,

else $P_{\text{start}} \leftarrow P_a; P_{\text{end}} \leftarrow P_c$.

Step 6. Translate $P_{\text{start}} = (0, 0)$, rotate triangle such that $P_b = (-X, 0)$ for $\alpha > 1$; $P_b = (X, 0)$ for $\alpha \leq 1$.

If $P_{\text{end}} = (X, -Y)$ or $P_{\text{end}} = (-X, -Y)$, then reflect the triangle through x -axis.

Step 7. Compute $\theta_d \leftarrow \pi - \cos^{-1}((- \|P_a P_c\|^2 + \|P_b P_c\|^2 + \|P_a P_b\|^2) / (2 \|P_b P_c\| \|P_a P_b\|))$.

Step 8. If $\alpha > 1$, then $\theta_f \leftarrow \cos^{-1}((- \|P_a P_b\|^2 + \|P_b P_c\|^2 + \|P_a P_c\|^2) / (2 \|P_a P_c\| \|P_b P_c\|))$,

else $\theta_e \leftarrow \cos^{-1}((- \|P_b P_c\|^2 + \|P_a P_b\|^2 + \|P_a P_c\|^2) / (2 \|P_a P_b\| \|P_a P_c\|))$.

Step 9. Identify bound of Λ . If $\alpha < 1$, then $a \leftarrow 1 \times 10^{-10}$; $b \leftarrow 1 / (\theta_d (1 - \alpha))$,

else if $\alpha > 1$, then $a \leftarrow 1 \times 10^{-10}$; $b \leftarrow 1 / (\theta_d (\alpha - 1))$,

else $a \leftarrow 1 \times 10^{-10}$; $b \leftarrow 1 \times 10^5$.

Step 10. Set tolerance $\text{Tol} \leftarrow 10^{-10}$;

iteration number $N \leftarrow (1 / \ln 2) \ln(|a - b| / \text{Tol})$.

Step 11. Calculate Λ using Bisection method.

Step 12. Determine scaling factor, $r_{\text{scale}} \leftarrow \|P_a P_c\| / \|P_0 P_2\|$.

Step 13. Scale r_{scale} to the curve and transform inversely the triangle to its original position.

Step 14. Construct LAC segment using (2).

Step 15. OUTPUT $(\theta_d, \Lambda, r_{\text{scale}}$, LAC segment).

End

ALGORITHM 1

the intersection point of the tangential line at both endpoints by solving the equations simultaneously.

2.2.3. Affirmation of Initial and Last Point Position (Step 5). We assume the distance between P_a and P_b is less than P_b and P_c as proposed by Yoshida and Saito [10]. The position of P_a and P_c is switched if the criterion is not satisfied. Otherwise, the position remains unchanged. Note that there are two cases of constructing LAC segment based on the α value as illustrated in Figures 2 and 3. For case $\alpha \leq 1$, the initial endpoint P_a is the starting point during the curve construction process P_{start} . On the other hand, starting point of curve construction process for case $\alpha > 1$ is the last endpoint P_c .

2.2.4. Transformation Process (Step 6). The transformation process includes translation, rotation, and reflection of the original triangle that consist of P_a, P_b, P_c . Initially, the original triangle is translated to the origin so that the starting point P_{start} is located at the origin. Next, we rotate the triangle so that the second control point is placed on the x -axis. Finally, we ensure the last point of the curve construction process P_{end} is located at the positive y -axis region. If not, the reflection process is needed to reflect the last point with

negative y -coordinate through the x -axis. The configuration after transformation is illustrated in Figures 2 and 3.

2.2.5. Computation of Tangent and Turning Angle (Step 7 and Step 8). We apply the law of cosine of a triangle to calculate corresponding angles as shown in Figures 2 and 3. The tangent angle θ_d and turning angle θ_e for case $\alpha \leq 1$ or θ_f for case $\alpha > 1$ will be used in the subsequent step for calculating shape parameter Λ .

2.2.6. Upper Bound of Shape Parameter Λ (Step 9). For the case when $\alpha = 1$, there is no upper bound for shape parameter Λ . So, the value of Λ can be arbitrarily large. However, there are upper bounds for Λ when $\alpha < 1$ and $\alpha > 1$. Therefore, the Λ value of these two cases is restricted within the range of (a, b) where a and b are assigned a specified value as indicated in the algorithm above.

2.2.7. Shape Parameter Λ Calculation (Step 10 and Step 11). We determine the Λ value that satisfies the constraints of endpoints and angles by using bisection method. First, tolerance and bound of Λ are used in the calculation of iteration number for bisection method. Then, the calculating process will run until the iteration number is met. Once the Λ



(a) Euler spiral algorithm

(b) LAC algorithm with two tangents setting for s-shaped curve and $\alpha = -1$ (c) LAC algorithm with two tangents setting for s-shaped curve and $\alpha = 2$

FIGURE 5: The results of fitting Euler spiral and LAC segment for two missing parts of a jug.

value of the curve is obtained, it is an interpolating curve that satisfies boundary constraints as shape parameter Λ is used to control the curve so that the constraints are satisfied. The obtained Λ value ensures the generated LAC segment starts at the starting point and ends at the last point while the shape of curve follows the specified tangent vectors at two endpoints.

2.2.8. Computation of Scale Factor (Step 12). We calculate the scaling factor by using the formula as shown in the algorithm where P_a and P_c are endpoints of the original triangle while P_0 and P_2 are endpoints of the transformed triangle.

2.2.9. Construction of LAC Segment (Step 13–Step 15). In order to obtain the curve which is defined in the original triangle, we inversely transform the triangle to its original position.

The curve segment is constructed using (2) with the obtained value of $\Lambda, \theta_d, r_{scale}$.

3. Numerical Examples and Discussion

This section shows the input data and numerical and graphical results of implementing the algorithm presented in Section 2 for three examples. For comparison purpose, we present the results of Kimia's algorithm [3] algorithm on the same examples as well.

3.1. The Graphical Results. Figure 5 shows the first example of fitting Euler spiral and LAC segment to two parts of a jug. The results of the second example (artifact) and third example (vase) are depicted in Figures 6 and 7, respectively.

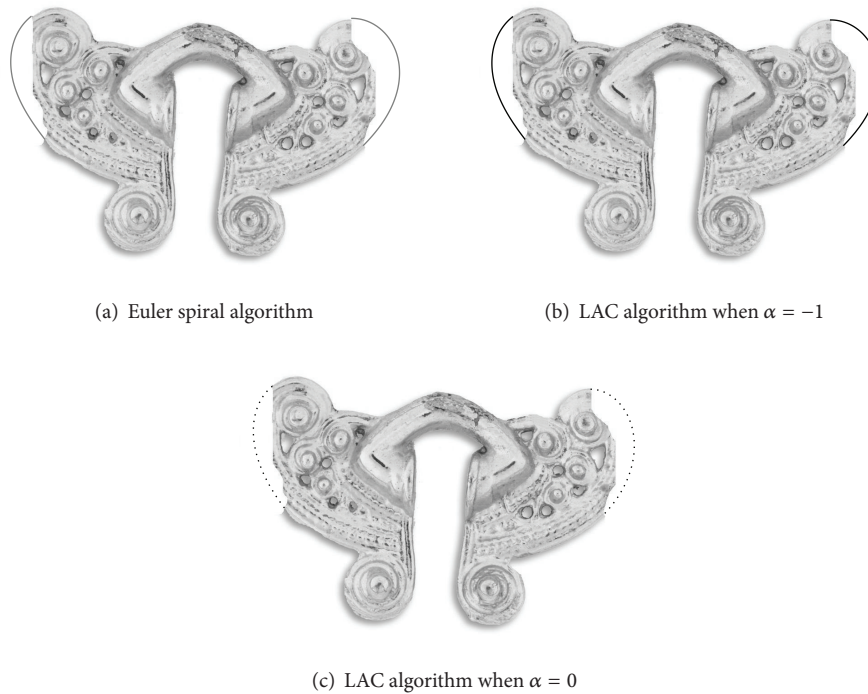


FIGURE 6: The results of fitting Euler spiral and LAC segment for an artifact.

3.2. *The Numerical Results.* The input data and the obtained parameter values to render LAC segment for C-shaped and S-shaped gaps are shown in Tables 1, 2, and 3, respectively.

3.3. *Discussion.* We implemented LAC algorithm with various α values for each example. In Figures 5, 6, and 7, we showed a subfigure of LAC with $\alpha = -1$ in between the gaps for the missing part of the objects. These examples are indeed Euler spiral similar to the work of Kimia et al. [3]. Users are indeed fitting a circle involute when $\alpha = 2$ as shown in each figure; Nielsen spiral is fitted when $\alpha = 0$ and logarithmic spiral when $\alpha = 1$. The shape parameter α definitely dictates the type of spiral the user desires to fit into the gap.

Based on the comparison of graphical results in Figures 5, 6 and 7 we found that Kimia's algorithm [3] and the LAC algorithm behave similarly. However, the proposed LAC algorithm gives more flexibility to designers as they can manipulate the shape parameter α and the tangent direction at the inflection point in order to get various S-shaped LAC segments.

4. Conclusion

A LAC segment can be constructed by specifying the endpoints and their tangent directions. LAC is a family of aesthetic curves where their curvature changes monotonically. It comprises Euler spiral, logarithmic spiral, Nielsen spiral, and circle involute with different α values. The algorithm for constructing LAC segment to solve shape completion

problem is defined in Section 2. The results of implementing both Kimia et al.'s [3] algorithm and the proposed LAC algorithm on the same images are depicted in Section 3. LAC has an upper hand due to its flexibility although both algorithms are capable of solving shape completion problems. Since LAC represents a bigger family rather than Euler spiral alone, it is clear that more shapes are available to fill the missing gap. Moreover, the resulting LAC segments are satisfying G^1 continuity where the curve segments interpolate both endpoints in the specified tangent directions. In case the user wants a G^2 LAC solution, one may plug in the technique proposed by Miura et al. [15] or employ G^2 GLAC [17] in which we may use shape parameter ν in GLAC to satisfy the desired curvatures.

Conflict of Interests

The authors declare that there is no conflict of interests regarding the publication of this paper.

Acknowledgments

The authors acknowledge Universiti Malaysia Terengganu (GGP grant) and Ministry of Higher Education Malaysia (FRGS: 59265) for providing financial aid to carry out this research. They further acknowledge anonymous referees for their constructive comments which improved the readability of this paper.

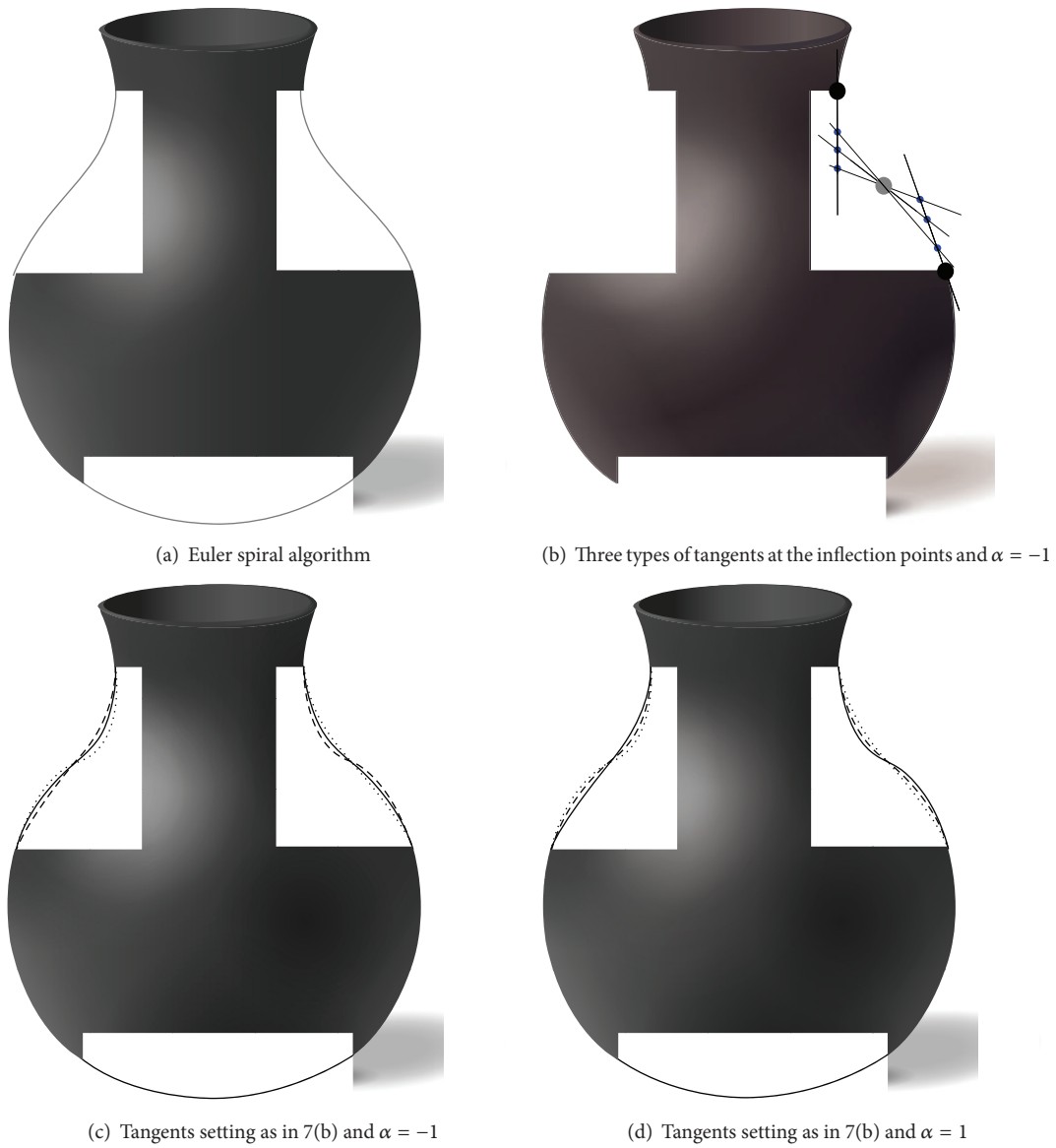


FIGURE 7: The results of fitting Euler spiral and LAC segment to a vase.

TABLE 1: The input data for LAC algorithm.

Figure	Part/gap shape	Starting point P_a	Inflection point P_{inflect}	Terminating point P_c
Figure 5	Outer C	(475.33, 290.67)	—	(408, 512)
	Inner C	(444, 319.3)	—	(406.7, 490.7)
	S	(68.67, 198)	(115.139, 317.874)	(132, 445.33)
Figure 6	Left C	(150.4, 320.8)	—	(123.2, 589.6)
	Right C	(853, 307)	—	(824, 583)
Figure 7	C	(504, 126)	—	(176, 120)
	Right S	(576.67, 379.33)	(501.722, 483.092)	(445.33, 598)
	Left S	(215.33, 599.33)	(166.565, 481.2)	(94, 376)

TABLE 2: The value of parameters obtained in LAC algorithm for C-shaped gap.

Figure	Part	Shape parameter	Angles (radian)		Scale factor
		Λ	θ_d	θ_e or θ_f	r_{scale}
Figure 5(b)	Outer C	0.181102	1.97352	1.09383	106.443
	Inner C	0.187822	2.50305	1.53612	57.7559
Figure 5(c)	Outer C	0.236827	1.97352	0.879684	179.903
	Inner C	0.307163	2.50305	0.966927	144.024
Figure 6(b)	Left C	0.319685	1.55147	1.00107	105.562
	Right C	0.204861	2.35562	1.47579	89.6424
Figure 6(c)	Left C	0.53364	1.55147	1.00107	90.2434
	Right C	0.610563	2.35562	1.47579	65.4159
Figure 7(c)	—	0.140054	1.1637	0.601359	271.762
Figure 7(d)	—	0.169061	1.1637	0.601359	270.036

TABLE 3: The value of parameters obtained in LAC algorithm for S-shaped gap.

Figure	Part	Line style	Shape parameter	Angles (radian)		Scale factor	
			Λ	θ_d	θ_e or θ_f	r_{scale}	
Figure 5(b)	—	Piece 1	Thick	0.646746	0.739623	0.451367	107.501
			Dashed	1.13587	0.43963	0.288258	152.739
		Piece 2	Thick	0.140372	1.32647	0.689653	93.5698
			Dashed	0.473033	1.02648	0.63682	76.6964
Figure 5(c)	—	Piece 1	Thick	2.19523	0.43963	0.151372	568.396
			Dashed	1.07216	0.739623	0.288256	293.721
		Piece 2	Thick	0.811123	1.02648	0.389659	222.587
			Dashed	0.156681	1.32647	0.63682	116.479
Figure 7(c)	Right S	Piece 1	Thick	0.0000429688	0.571501	0.285752	227.044
			Dashed	0.698712	0.871501	0.585746	39.271
			Dotted	2.45758	0.371528	0.285746	23.657
		Piece 2	Thick	0.0118778	0.908437	0.455056	145.074
			Dashed	0.403597	1.20905	0.755673	65.1694
			Dotted	0.700923	0.707704	0.45338	100.657
Figure 7(d)	Right S	Piece 1	Thick	2.53147	0.871501	0.585746	41.1231
			Dashed	0.0000429592	0.571501	0.285752	227.044
			Dotted	10.7779	0.371528	0.285746	25.7032
		Piece 2	Thick	1.2606	1.20905	0.755673	47.4646
			Dashed	0.0120078	0.908437	0.455056	145.071
			Dotted	2.48785	0.707704	0.45338	67.3212
Figure 7(c)	Left S	Piece 1	Thick	0.188412	0.981157	0.509674	121.657
			Dashed	0.603719	0.781142	0.471473	103.99
			Dotted	0.361402	1.38114	0.909666	52.4523
		Piece 2	Thick	0.0000462514	0.594672	0.297337	218.104
			Dashed	0.884532	0.394671	0.297335	35.514
			Dotted	0.564167	0.994666	0.697331	27.5123
Figure 7(d)	Left S	Piece 1	Thick	1.61781	0.781142	0.471473	83.3887
			Dashed	0.234412	0.981157	0.509674	120.616
			Dotted	1.42816	1.38114	0.909666	31.5215
		Piece 2	Thick	9.26646	0.394671	0.297335	31.4849
			Dashed	0.0000462423	0.594672	0.297337	218.104
			Dotted	2.66752	0.994666	0.697331	26.6104

References

- [1] M. Kolomenkin, I. Shimshoni, and A. Tal, “Demarcating curves for shape illustration,” *ACM Transactions on Graphics*, vol. 27, no. 5, article 157, 2008.
- [2] D. Decarlo, A. Finkelstein, S. Rusinkiewicz, and A. Santella, “Suggestive contours for conveying shape,” *ACM Transactions on Graphics*, vol. 22, no. 3, pp. 848–855, 2003.
- [3] B. B. Kimia, I. Frankel, and A. Popescu, “Euler spiral for shape completion,” *International Journal of Computer Vision*, vol. 54, no. 1–3, pp. 159–182, 2003.
- [4] T. Judd, F. Durand, and E. Adelson, “Apparent ridges for line drawing,” *ACM Transactions on Graphics*, vol. 26, no. 3, article 19, 7 pages, 2007.
- [5] S. Yoshizawa, A. Belyaev, and H. P. Seidel, “Fast and robust detection of crest lines on meshes,” in *Proceedings of the ACM Symposium on Solid and Physical Modeling (SPM '05)*, pp. 227–232, June 2005.
- [6] G. Harary and A. Tal, “3D Euler spirals for 3D curve completion,” *Computational Geometry: Theory and Applications*, vol. 45, no. 3, pp. 115–126, 2012.
- [7] I. Kanaya, Y. Nakano, and K. Sato, “Simulated designer’s eyes—classification of aesthetic surfaces,” in *Proceedings of the International Conference on Virtual Systems and Multimedia*, pp. 289–296, 2003.
- [8] R. U. Gobithaasan and K. T. Miura, “Logarithmic curvature graph as a shape interrogation tool,” *Applied Mathematical Sciences*, vol. 8, no. 16, pp. 755–765, 2014.
- [9] K. T. Miura, J. Sone, A. Yamashita, and T. Kaneko, “Derivation of a general formula of aesthetic curves,” in *Proceedings of 8th International Conference on Humans and Computers*, pp. 166–171, Tokyo, Japan, 2005.
- [10] N. Yoshida and T. Saito, “Interactive aesthetic curve segments,” *The Visual Computer*, vol. 22, no. 9–11, pp. 896–905, 2006.
- [11] R. U. Gobithaasan and K. T. Miura, “Aesthetic spiral for design,” *Sains Malaysiana*, vol. 40, no. 11, pp. 1301–1305, 2011.
- [12] J. M. Ali, R. M. Tookey, J. V. Ball, and A. A. Ball, “The generalised Cornu spiral and its application to span generation,” *Journal of Computational and Applied Mathematics*, vol. 102, no. 1, pp. 37–47, 1999.
- [13] R. U. Gobithaasan, R. Karpagavalli, and K. T. Miura, “Shape analysis of generalized log-aesthetic curves,” *International Journal of Mathematical Analysis*, vol. 7, no. 33, pp. 1751–1759, 2013.
- [14] R. Ziatdinov, N. Yoshida, and T. Kim, “Analytic parametric equations of log-aesthetic curves in terms of incomplete gamma functions,” *Computer Aided Geometric Design*, vol. 29, no. 2, pp. 129–140, 2012.
- [15] K. T. Miura, D. Shibuya, R. U. Gobithaasan, and S. Usuki, “Designing log-aesthetic splines with G^2 continuity,” *Computer-Aided Design and Applications*, vol. 10, no. 6, pp. 1021–1032, 2013.
- [16] K. T. Miura and R. U. Gobithaasan, “Aesthetic curves and surfaces in computer aided geometric design,” *International Journal of Automation Technology*, vol. 8, no. 3, pp. 304–316, 2014.
- [17] R. U. Gobithaasan, R. Karpagavalli, and K. T. Miura, “ G^2 continuous generalized log aesthetic curves,” *Computer Aided Design & Application*, Accepted for publication.